Front. Mech. Eng. 2017, 12(3): 357–366
DOI 10.1007/s11465-017-0423-4

RESEARCH ARTICLE

Xiaoli XU, Xiuli LIU

Weak characteristic information extraction from early fault of wind turbine generator gearbox

Abstract Given the weak early degradation characteristic information during early fault evolution in gearbox of wind turbine generator, traditional singular value decomposition (SVD)-based denoising may result in loss of useful information. A weak characteristic information extraction based on μ-SVD and local mean decomposition (LMD) is developed to address this problem. The basic principle of the method is as follows: Determine the denoising order based on cumulative contribution rate, perform signal reconstruction, extract and subject the noisy part of signal to LMD and μ-SVD denoising, and obtain denoised signal through superposition. Experimental results show that this method can significantly weaken signal noise, effectively extract the weak characteristic information of early fault, and facilitate the early fault warning and dynamic predictive maintenance.

Keywords wind turbine generator gearbox, μ-singular value decomposition, local mean decomposition, weak characteristic information extraction, early fault warning

1 Introduction

The extraction of fault characteristics is directly related to the veracity and reliability in mechanical fault diagnosis. Considering the weak early degradation characteristic information during the evolution of transmission system fault in wind turbine generator, the deterioration characteristic information is frequently consumed by such non-deterioration information as variable condition. Moreover, the large amount of noise in the vibration signal of wind turbine generator acquired with sensor may lead to low signal-to-noise ratio (SNR) and high complexity and diversity. These factors may seriously affect the extraction of deterioration state characteristic information. Effectively reducing the background noise in vibration signal and highlight state characteristic information is a key technique that affects the running state deterioration characteristic extraction for wind turbine [1–4].

In recent years, nonlinear filtering-based singular value decomposition (SVD) has been proven an effective signal processing tool that can extract the main characteristic components of signal and is thus being widely used for engineering signal processing [5–10]. The basic principle of traditional SVD denoising is as follows: Subject observation signal to phase space reconstruction; use SVD to decompose observation signal space into noisy signal subspaces and noise subspaces corresponding to a series of singular values; reserve several large singular values corresponding to noisy signal subspace, and set the rest of the singular values to zero; attain pure signal matrix estimate equation through SVD inverse process; and recover the denoised signal through phase space inverse reconstruction. Certain singular values reserved in traditional SVD denoising are principally associated with noise contribution, and the resulting pure signal matrix estimate equation contains much noise information. Accordingly, traditional SVD denoising cannot provide favorable effect of denoising under high noise.

Zeng et al. [11] proposed a universal SVD-based subspace denoising, that is, μ-SVD denoising algorithm. Traditional SVD denoising is only a special case of μ-SVD denoising when Lagrangian multiplier $\mu = 0$. When the μ value is properly chosen, μ-SVD denoising can provide better denoising effect as compared with traditional SVD denoising. However, considering that traditional SVD denoising and μ-SVD denoising "give up" a part of signal represented by singular value and that such part of signal may often contain useful information, especially in the signal acquired in the background of strong noise on site, the useful information in "given up" signal must be rationally extracted. Zhu et al. [12] used empirical mode

Received July 14, 2016; accepted December 6, 2016

Xiaoli XU, Xiuli LIU (✉)
Key Laboratory of Modern Measurement & Control Technology (Ministry of Education), Beijing Information Science and Technology University, Beijing 100192, China
E-mail: liuxiulilw@163.com

decomposition (EMD) in SVD denoising to extract the weak information for the terms that are "given up" in SVD denoising and contain weak useful information; the method is proven effective. Hence, this study proposes a weak characteristic information extraction based on μ-SVD and local mean decomposition (LMD) for early fault by introducing the highly optimized LMD [13–16] as compared with EMD into SVD denoising. The proposed method is then used to analyze vibration signal of wind turbine generator in a strong noise background and extract the weak characteristic information of deterioration state characteristic.

2 Weak characteristic information extraction

2.1 μ-SVD

μ-SVD denoising is developed by applying time-domain constraint estimate to SVD-based subspace denoising. Traditional SVD denoising is a special case of μ-SVD denoising when Lagrange multiplier $\mu = 0$. μ-SVD denoising involves filter value factor f_μ that filtrates the reserved singular values and suppresses the information contribution of noise contribution-dominated singular values to pure signal matrix estimate equation. μ-SVD denoising involves five parameters: Delay time τ, embedding dimension d, denoising order k, noise power σ_w^2, and Lagrange multiplier μ; these parameters determine the ultimate denoising effect.

The procedure of μ-SVD denoising is as follows:

1) Determine embedding dimension d and delay time τ, and subject observation signal x to phase space reorganization to obtain observation signal matrix $\boldsymbol{X}$.

2) Use SVD to decompose observation signal matrix $\boldsymbol{X}$, that is, $\boldsymbol{X} = \boldsymbol{U}\Sigma\boldsymbol{V}^{\mathrm{T}}$.

3) Determine denoising order k, and extract the first k column vectors of matrices $\boldsymbol{U}$, Σ, and $\boldsymbol{V}$ to obtain submatrices $\boldsymbol{U}_1$, Σ_1, and $\boldsymbol{V}_1$.

4) Determine noise power σ_w^2 and Lagrange multiplier μ for computing matrix $\boldsymbol{F}_\mu = (\boldsymbol{I}_k - \sigma_w^2\Sigma_1^{-2})(\boldsymbol{I}_k - (1-\mu)\sigma_w^2\Sigma_1^{-2})^{-1}$, $\boldsymbol{I}_k = \boldsymbol{U}^{\mathrm{T}}\boldsymbol{U}$.

5) Calculate the estimated pure signal matrix $\hat{\boldsymbol{S}}_\mu = \boldsymbol{U}_1\boldsymbol{F}_\mu\Sigma_1\boldsymbol{V}_1^{\mathrm{T}}$, and obtain the denoised signal through phase space inverse reconstruction of $\hat{\boldsymbol{S}}$.

The procedures for determining the abovementioned parameters of μ-SVD denoising are provided as follows.

1) Delay time

Phase space reconstruction delay time is a key parameter. Delay time is determined with extensively used mutual information function (MIF) [17] and is defined as

$$D(\tau) = \sum_{i=1}^{N-\tau} p(x_i, x_{i+\tau}) \ln \frac{p(x_i, x_{i+\tau})}{p(x_i)p(x_{i+\tau})}, \quad (1)$$

where $p(x_i)$, $p(x_{i+\tau})$, and $p(x_i, x_{i+\tau})$ represent probability. This study uses the τ value corresponding to the first minimum of MIF as the delay time τ_0.

2) Embedding dimension

Embedding dimension d is another important parameter of phase space reconstruction. Cao [18] proposed an improved false nearest neighbor point method that determines phase space reconstitution embedding dimension. The method is expressed as follows:

$$E(d) = \frac{1}{N - d\tau} \sum_{i=1}^{N-d\tau} \frac{\|\boldsymbol{X}_i(d+1) - \boldsymbol{X}_{n(i,d)}(d+1)\|}{\|\boldsymbol{X}_i(d) - \boldsymbol{X}_{n(i,d)}(d)\|}, \quad (2)$$

where $\boldsymbol{X}_i(d)$ represents the ith reconstructed vector with embedding dimension equal to d; $\boldsymbol{X}_{n(i,d)}(d)$ is the nearest neighbor point of $\boldsymbol{X}_i(d)$. When delay time τ is determined, $E(d)$ is dependent on embedding dimension d only.

The ratio is defined as

$$E_1(d) = \frac{E(d+1)}{E(d)}. \quad (3)$$

The d value obtained when d is slowly increased to $E_1(d)$ is the minimum embedding dimension. No clear criterion is currently available for determining $E_1(d)$ through slow variation. Hence, a maximum embedding dimension $d_{\max}$ is provided and gradually increased by d until the $E_1(d)$ values of all subsequent points vary within the given range Δ, when the corresponding d value is the minimum embedding dimension d_0 .

3) Denoising order

In general, evaluating the denoising order k is necessary in practice. The large singular k values in the front of singular value sequence $\{\sigma_i\}$ ($i = 1, 2, \ldots, d$) are jointly contributed by pure signal and noise, while the remaining singular $d-k$ values are entirely contributed by noise. Singular value cumulative contribution rate is used to determine denoising order in this study. Singular value is corrected based on the following equation:

$$\sigma_i' = \sqrt{\sigma_i^2 - \sigma_d^2},\ i = 1, 2, \ldots, d.$$

The singular value cumulative contribution rate after correction is

$$\eta = \frac{\sum_{i=1}^{k} \sigma_i'}{\sum_{i=1}^{d} \sigma_i'} \times 100\%. \quad (4)$$

The k value obtained when cumulative contribution rate η reaches 80%–90% can normally be used as denoising

order k_0.

4) Noise power

In the event of ideal noise, all singular values contributed by noise are completely equal to one another. In practice, these singular values are not completely equal to one another but exhibit a slowly decreasing distribution. Accordingly, the mean value of these singular values can be used to estimate noise power. When denoising order is identified as k, the noise power estimation equation is

$$\sigma_{\mathrm{w}}^2 = \frac{1}{d-k}\sum_{i=k+1}^{d}\sigma_i^2. \tag{5}$$

5) Lagrange multiplier

Lagrange multiplier μ determines the final effect of μ-SVD denoising to a large extent. The selection of Lagrange multiplier μ in μ-SVD denoising considers the following empirical principles: The relatively small μ value can be selected for signal with high SNR. Appropriate μ value is ideally near $\mu = 1$.

2.2 Local mean decomposition

LMD is adaptive decomposition based on the signal itself. Each product function (PF) component attained is physically significant, reflects the intrinsic nature of signal, and features strong adaptability and low computing load.

LMD decomposes a complex signal into the sum of a finite number of PF components, such that the characteristic information of original signal is extracted. Therefore, any signal $x(t)$ should be subjected to LMD decomposition as shown in Fig. 1 to obtain PF component.

2.3 Weak characteristic information extraction

2.3.1 Rationale

The rationale of weak characteristic information extraction based on μ-SVD and LMD is identified on the basis of the analysis above as follows: Build Hankel matrix for original signal containing strong noise, and determine the denoising order based on cumulative contribution rate of singular value; decompose that matrix into two parts through SVD decomposition, that is, the diagonal matrix containing effective singular value, and the diagonal matrix constructed using the remaining singular values with the effective singular values set to zero, as shown in Eq. (6).

$$\begin{aligned}\boldsymbol{H}_{m\times n} &= \boldsymbol{U}\boldsymbol{\Sigma}\boldsymbol{V}^{\mathrm{T}} \\ &= \boldsymbol{U}\begin{pmatrix}\Lambda_1 & 0\\ 0 & 0\end{pmatrix}\boldsymbol{V}^{\mathrm{T}} + \boldsymbol{U}\begin{pmatrix}0 & 0\\ 0 & \Lambda_2\end{pmatrix}\boldsymbol{V}^{\mathrm{T}}.\end{aligned} \tag{6}$$

The part containing effective singular value must be reversed to obtain useful signal with faint noise; the reversal of the other part introduces residual terms that contain useful signal. Hence, it is reconstructed into a new Hankel matrix and reversed to obtain original signal component under weak signal and strong noise. SNR is enhanced through LMD, while the noise is substantially found in a few effective PF; these PFs are denoised through μ-SVD, and the PF signal component is reconstructed. The reconstructed PF components and the remaining PF components are superposed to obtain faint useful signal. When the requirement is still not satisfied, then the abovementioned process can be repeated for cyclic decomposition of such weak signal until the effective signal is attained. Finally, the first part of useful signals and the said weak effective signal are reconstructed to obtain original information.

2.3.2 Method and process

The flow chart of the method for weak characteristic information extraction is shown in Fig. 2.

The weak characteristic extraction based on μ-SVD and LMD is realized in the following procedure:

1) Build $m \times n$-dimension Hankel matrix and perform SVD for noisy signal $x(t)$, determine the effective singular value, and decompose original signal with noise into two parts using Eq. (6).

2) The first part of signal reconstruction obtains superposed signal $x_1(t)$, and the second part of reconstruction obtains signal $x_2(t)$ with noise.

3) Subject $x_2(t)$ to LMD decomposition, use effective PF component to perform μ-SVD based signal denoising, and superpose the denoised PF component and the rest of PF components to weak information $x_3(t)$.

4) Superpose $x_1(t)$, $x_3(t)$, and trend term to obtain denoised signal $x'(t)$.

5) When denoised signal fails to satisfy the requirements, repeat steps 3) and 4) until effective signal is extracted.

In this process, effective PF is selected in determining the correlation of each PF with original signal; the correlation ρ_i computing method described in Ref. [19] is used to distinguish useful component from false PF component. The correlation value of each PF component with original signal is calculated; if the correlation ρ_i of a certain PF component with original signal is below the preset threshold λ, then it must be eliminated as false component. λ can be used as a ratio of maximum correlation and is expressed as follows:

$$\lambda = \max(\rho_i)/\eta, i = 1,2,...,n,$$

where η represents a proportionality constant with a value larger than 1. The correlation between sequences $x(n)$ and $y(n)$ is expressed as

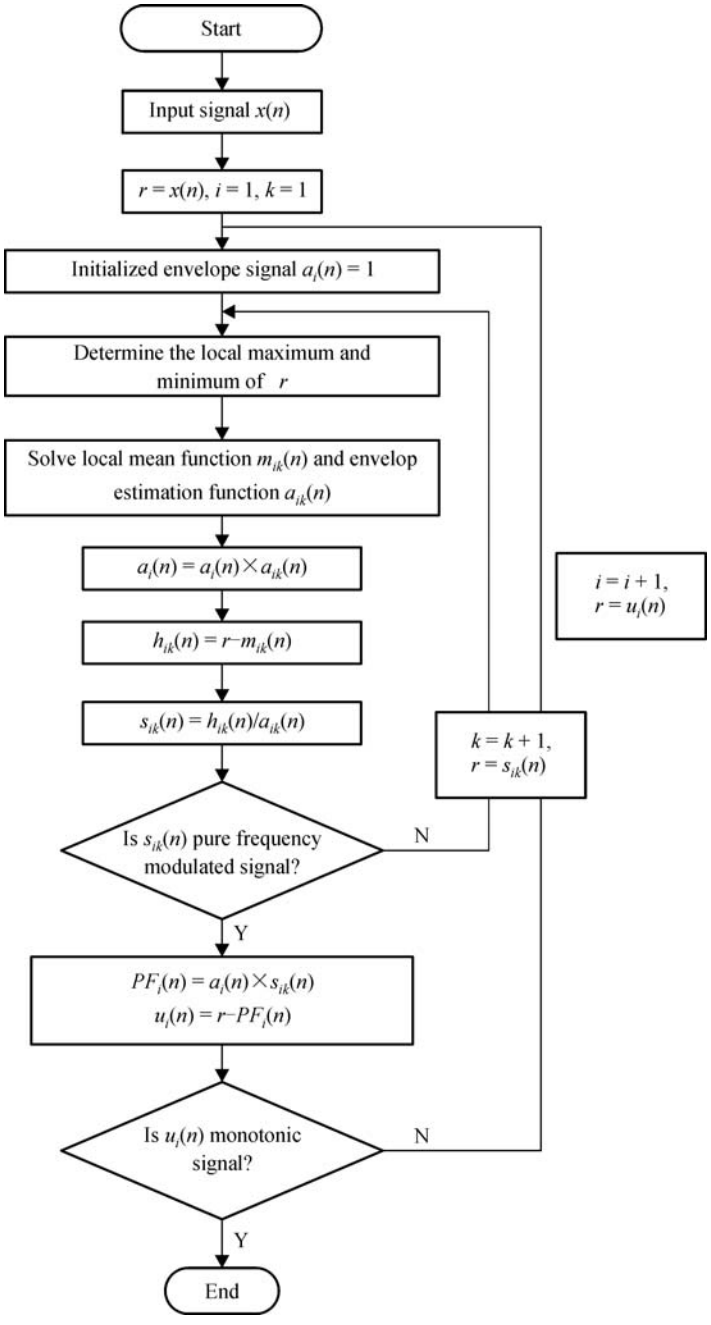

Fig. 1 LMD algorithm flow chart

$$\rho_{xy} = \frac{\sum_{n=0}^{\infty} x(n)y(n)}{\sqrt{\sum_{n=0}^{\infty} x^2(n) \sum_{n=0}^{\infty} y^2(n)}}.$$

3 Simulation verification

The simulation signal is constructed as follows: The sine signal modulated by the fundamental frequency is 70 Hz, and the signal is modulated by the sine signal of 5 Hz, which is a sine signal with the frequency of 120 Hz. The expression is as follows:

$$X = 0.7\sin\Big(140\pi t + \cos(10\pi t)\Big) + \sin(240\pi t).$$

Figure 3 shows source signal of time- and frequency-domain waveforms. The waveforms show clear periodicity, and amplitude spectrum contains frequency of 70 Hz and side band frequency interval for 5 Hz. Amplitude

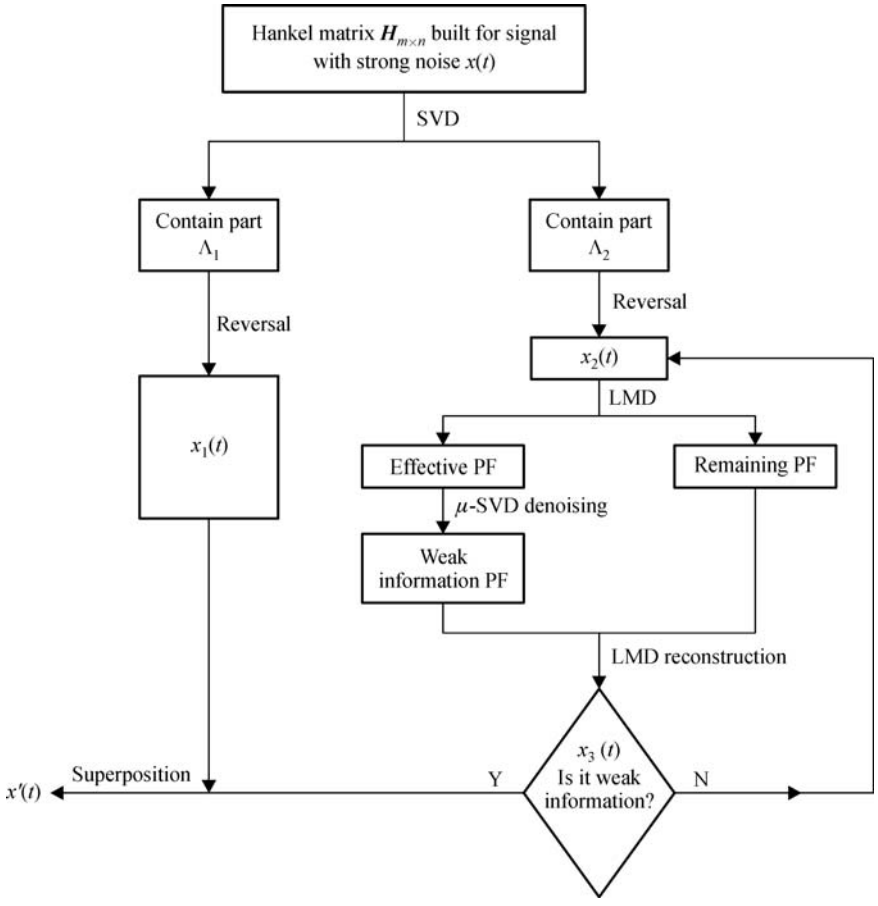

Fig. 2 Pretreatment method flow chart

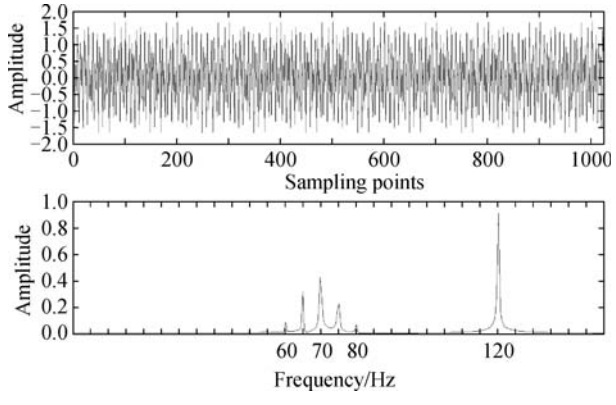

Fig. 3 Time-domain waveform and frequency spectrum of source signal

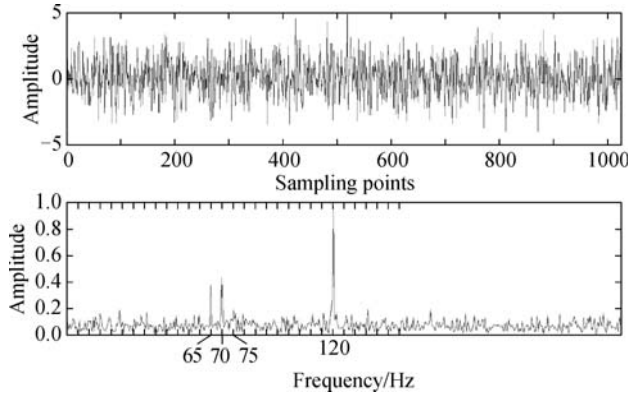

Fig. 4 Time-domain waveform and frequency spectrum of signal with noise

declines from the dominant frequency of 70 Hz to both sides, indicating that the signal of 70 Hz is modulated by the sinusoidal signal of 5 Hz. Spectrum is clean with no other interference frequency components.

White noise is added to the source signal. Figure 4 shows the time-domain waveform and frequency spectrum of the actual observation signal. Given the noise interference, some characteristics of the source signal are submerged, and the time-domain periodicity becomes insignificant. The frequencies of 65, 70, and 120 Hz are still significant but do not form the side band. A source signal in two main frequencies of 65 and 70 Hz exist at the same time.

The signal with noise is subjected to phase space

reconstruction, and the singular value is calculated. The cumulative contribution rate (CCR) of singular value is calculated, and the denoising order in the aforementioned way is determined to obtain denoising order.

As shown in Fig. 5, the cumulative contribution rate decreases below 85% when denoising order is 5, such that the denoising order k is identified as 4. The first four singular values are used as effective singular values and are decomposed into two parts using Eq. (6).

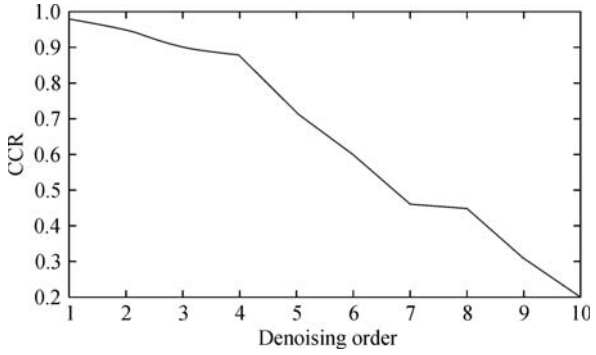

Fig. 5 Relation between denoising order and cumulative contribution rate (CCR)

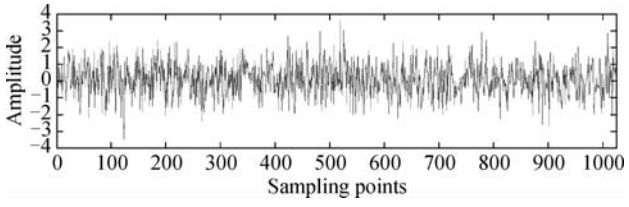

Fig. 6 Waveform of the second part of signal

Figure 6 shows that the second part of signals is messy and may contain useful information. However, further processing is needed owing to the weakness of useful information and the strong noise interference. The second part of signals is decomposed using LMD to attain three PF components and one residual component shown in Fig. 7.

The correlation of each of the three PF components with the second part of signals is calculated; the detailed numerical values are shown in Fig. 8.

A PF component with extremely low correlation is removed, and the remaining two PF components are subjected to weak characteristic information extraction based on μ-SVD. PF1 is used as an example in describing the denoising process in detail below.

The delay time τ needs to be determined first. As shown in Fig. 9, the τ value corresponding to the first minimum of MIF is considered the delay time τ_0, $\tau_0 = 2$.

To determine the embedding dimension d, a maximum embedding dimension $d_{\max}$ is given and gradually increased by d until the $E_1(d)$ values of all subsequent points vary within the given range Δ, when the corresponding d value is the minimum embedding dimension d_0. In this study, $d_{\max} = 20$, and $\Delta = 0.05$. As shown in Fig. 10, the embedding dimension $d_0 = 9$.

The k value obtained when CCR η reaches 80%–90% can be regarded as the denoising order k_0. As shown in Fig. 11, the denoising order $k_0 = 9$. In this study, the denoising order is identified as $k = 9$, and the calculated noise power $\sigma_w = 10820$. μ is determined based on the principle for selection of $\mu = 0.9$.

PF1 is subjected to weak characteristic information extraction based on μ-SVD, and the weak information is obtained and shown in Fig. 12. PF2 is subjected to weak characteristic information extraction based on μ-SVD

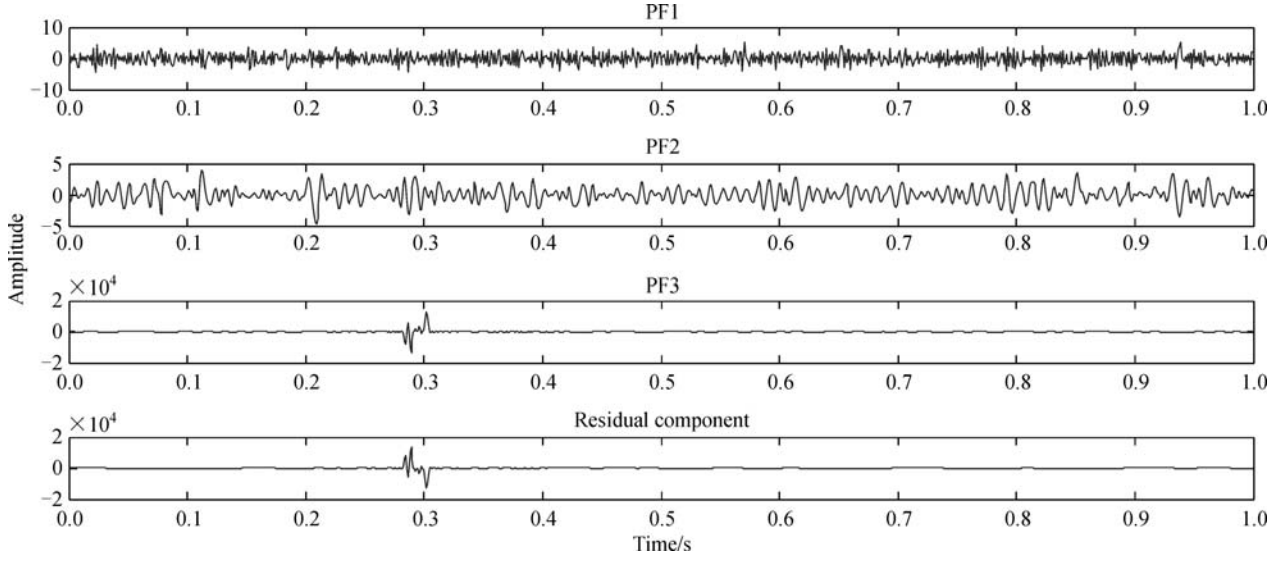

Fig. 7 LMD decomposition result of the second part of signals

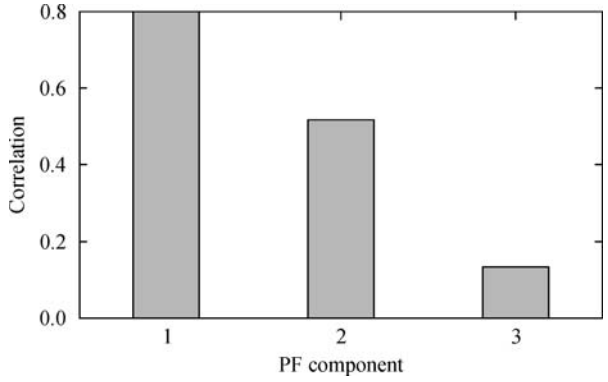

Fig. 8 Correlation of three PF components with the second part of signals

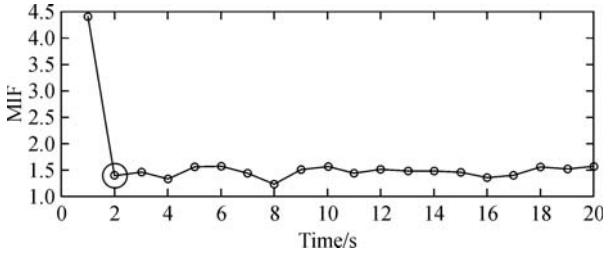

Fig. 9 Determination of delay time

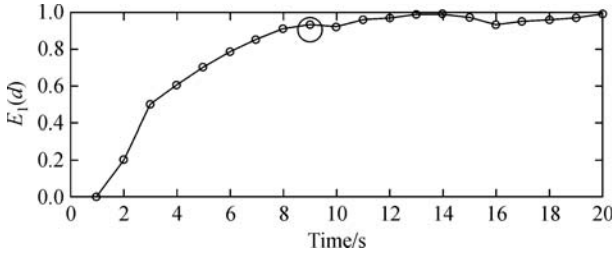

Fig. 10 Detemination of embedding dimension

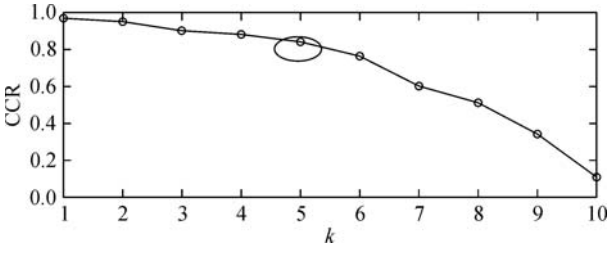

Fig. 11 Denoising order of phase space reconstruction

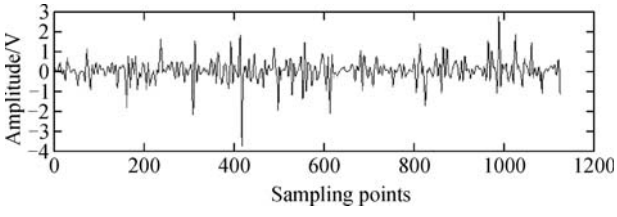

Fig. 12 Signal after extraction of weak information with PF1

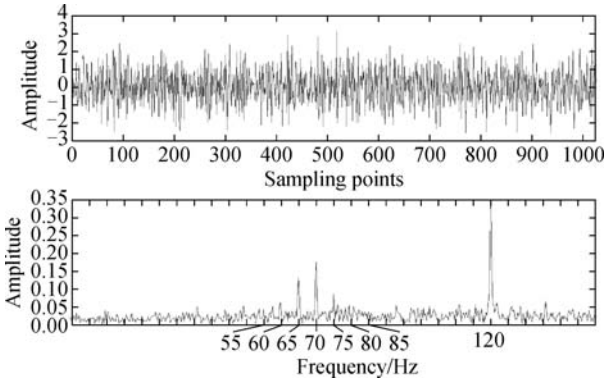

Fig. 13 Signal after extraction of weak information

using the same method as used for PF1, and it is superposed with the rest of the PF components and residual terms to obtain denoised second part of signals; the first and second parts of signals are then superposed to attain the weak information of signal as shown in Fig. 13.

As shown in Fig. 13, the noise energy is suppressed to a certain extent. The frequency signals of 60, 65, and 75 Hz (nearby 70 Hz) are extracted. The source signal in the presence of the frequency signal of 70 Hz is modulated by the sine signal component of 5 Hz. The simulation results show that, after the process with this method, and the noise in the spectrum is filtered out to a certain extent. As a consequence, the failure frequency characteristics are extracted with ease.

The weak characteristic information extraction spectrum indicates that the proposed weak signal extraction method can effectively extract all frequency components. Original signal is subjected to strong noise to weaken information extraction using SVD denoising and μ-SVD denoising. The comparison results between corresponding SNR and RMSE (root mean square error) are shown in Table 1.

Table 1 SNR and RMSE after treatment using different methods

Processing method	SNR/dB	RMSE
Weak characteristic information extraction	27.492	0.063
SVD denoising	26.871	0.079
μ-SVD denoising	27.426	0.077

Weak characteristic information extraction based on μ-SVD and LMD exhibits excellent noise suppression performance in terms of waveform, frequency spectrum, SNR, and RMSE after simulation signal noise suppression. Thus, this method can be used to pretreat state characteristic weak information of wind turbine generator.

4 Experimental verification

As a rotary device with high transmission ratio and power,

the gearbox in the transmission system of a wind turbine generator has to constantly bear varying wind loads and other loads; a large amount of data indicate that gearbox is a weak section in the transmission system of a wind turbine generator [20,21]. In consideration of its practical operational complexity, a wind power speed-up gearbox experiment table is established and used to verify the effectiveness of the method based on vibration data obtained at experiment table. Figure 14 shows the sensor arrangement.

Fig. 14 Installation locations of sensors

In the experiment, the type of rolling bearing is SKF6205 deep groove ball bearings, single point damage is produced by electric discharge machining, the damage diameter is 0.1778 mm, and depth is 0.2794 mm. Under a load of 0.74 kW inner ring fault, outer ring fault, and rolling body fault data are obtained. The sampling frequency is 12 kHZ, and the data length is 4096. Figure 15 shows the time-domain waveform.

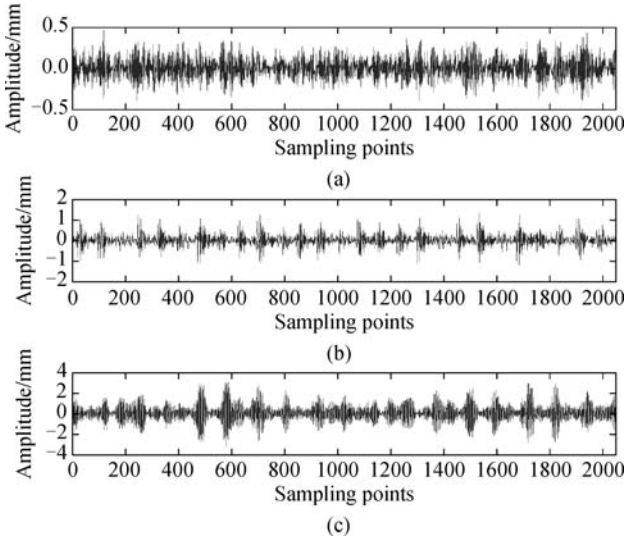

Fig. 15 Time-domain waveform of three kinds of faults. (a) Ball failure; (b) inner ring fault; (c) outer ring fault

The fault data of the three kinds of states present certain regularity, and the periodic impulse characteristics of the fault signal of the inner and outer races are obvious.

The experimental bearing speed is 1773 r/min. According to the rolling bearing geometry in Table 2, the frequency calculation of the type of deep groove ball bearing fault is conducted. The faults of rolling body, inner ring, and outer ring are 139.28, 160.02, and 105.93 Hz, respectively. The cage failure is 11.77 Hz.

Figure 16 shows the fast Fourier transform of the three sets of signals. The fault frequency is submerged in the noise and is thus difficult to be extracted. The vibration acceleration signal must be processed first to find the fault characteristic frequency. Thus, the experimental data are pretreated in each operating state of wind power speed-up gearbox using weak characteristic information extraction based on μ-SVD and LMD.

For the outer ring fault signal, the calculated fault characteristic frequency is 105.93 Hz. Given the noise, the fault characteristic frequency of 107.36 Hz and its frequency multiplication are not obvious, and the fault feature is submerged in the noise. As a result, accurately identifying the fault is difficult.

After SVD of this group of signals, the second part of signals is decomposed using LMD to attain four PF components shown in Fig. 17. The relationship between the PF components (PF1, PF2, PF3, and PF4) and the original signal are 0.9963, 0.0271, 0.0024, and 0.0024, respectively.

PF1 and PF2 are subjected to weak characteristic information extraction based on μ-SVD, and they are superimposed with the rest of the PF components to obtain denoised second part of signals; the first and second parts of signals are then superposed to attain the weak information of signal as shown in Figs. 18 and 19.

The results show that, after noise reduction, the noise components in the spectrum are eliminated. The number of micro burr in the spectrum is also reduced. The highest amplitude frequency point shows that the highest energy component of the signal is 533.7 Hz. With the very close outer ring fault characteristic frequency of 5 double frequency 529.65 Hz, less than 0.8% error in the acceptance range is obtained. Therefore, the proposed theoretical method can effectively diagnose the fault signal of rolling bearing of wind turbine generator.

5 Conclusions

1) A weak characteristic information extraction based on

Table 2 Deep groove ball bearing specification information

Model	Diameter of inner ring/mm	Diameter of outer ring/mm	Rolling body diameter/mm	Contact angle/(°)	Number of rolling elements
6205	25.00122	51.99888	8.18180	0	9

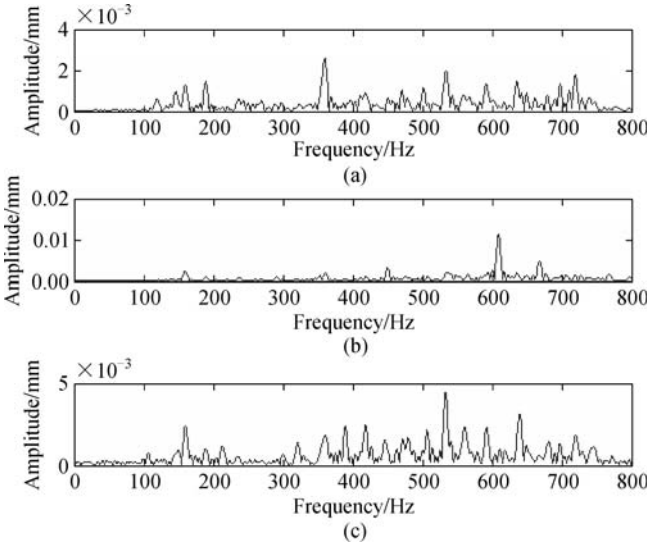

Fig. 16 Three kinds of fault signal spectrum. (a) Rolling body fault; (b) inner ring fault; (c) outer ring fault

μ-SVD and LMD is proposed for avoiding the consumption of weak early degradation characteristic information by such non-deterioration information as a variable condition during operation status deterioration of transmission system in wind turbine generator. The method is verified through simulation to identify its effectiveness. Pretreatment method for extraction of weak characteristic information from artificial signal is used, and the result of this method is compared with that of characteristic mean method and μ-SVD noise suppression. The simulation results indicate that the proposed signal preprocessing method can highlight state characteristic information.

2) Weak characteristic information extraction is used for analyzing vibration signal at wind power speed-up gearbox experiment table. The results show that the pretreated signal suppresses substantive background noise and retains the mutation component; hence, weak characteristic information extraction based on μ-SVD and LMD can pretreat the vibration signal of wind turbine generator. This study provides the basis for studying running state deterioration characteristic extraction.

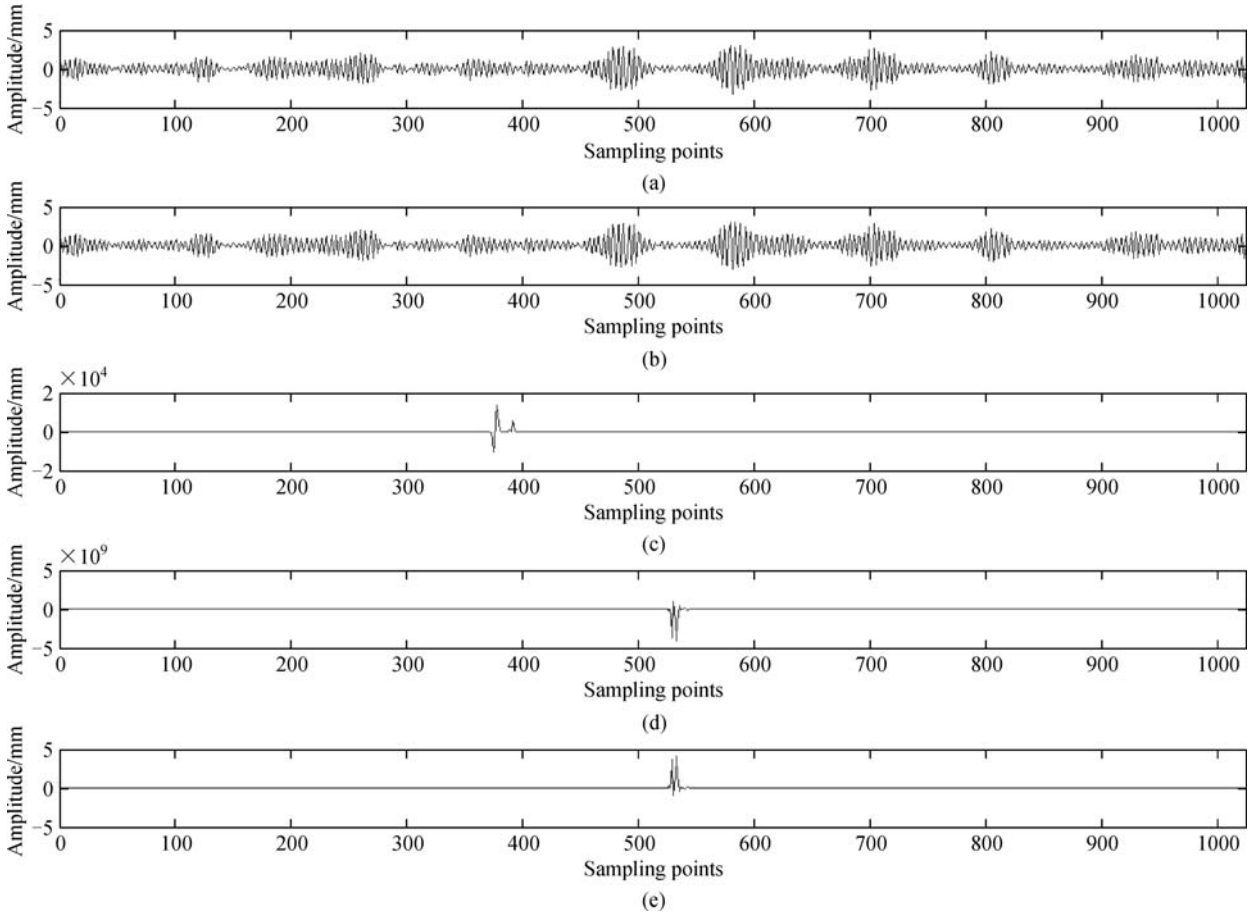

Fig. 17 Second part of the original signal and the PF component. (a) The second part of the original signal; (b) PF1; (c) PF2; (d) PF3; (e) PF4

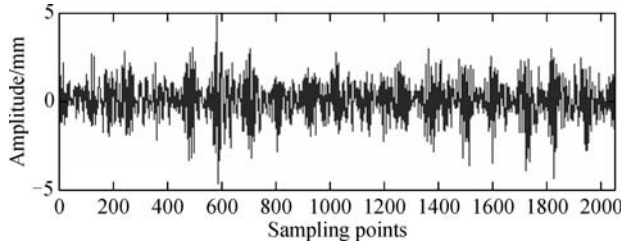

Fig. 18 Weak information of signal

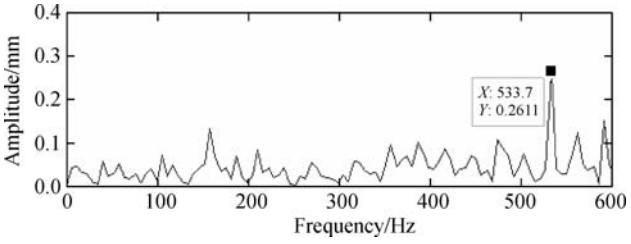

Fig. 19 Weak information spectrum

Acknowledgements This research was sponsored by the National Natural Science Foundation of China (Grant Nos. 51275052 and 51105041), and the Key Project Supported by Beijing Natural Science Foundation (Grant No. 3131002).

References

1. Wang G, He Z, Chen X, et al. Basic research on machinery fault diagnosis—What is the prescription. Journal of Mechanical Engineering, 2013, 49(1): 63–72 (in Chinese)
2. Xu X, Wang H. Large Rotating Machinery Running Trend Forecasting. Beijing: Science Press, 2011 (in Chinese)
3. Xu X, Jiang Z, Ren B, et al. Extract method of flue gas generator set state feature weak information based on Birgé-Massart threshold. Journal of Mechanical Engineering, 2012, 48(12): 7–12 (in Chinese)
4. Man Z, Wang W, Khoo S, et al. Optimal sinusoidal modeling of gear mesh vibration signals for gear diagnosis and prognosis. Mechanical Systems and Signal Processing, 2012, 33: 256–274
5. Lv Z, Zhang W, Xu J. A denoising method based singular spectrum and its application in machine fault diagnosis. Chinese Journal of Mechanical Engineering, 1999, 35(3): 85–88
6. Chen J, Zhang L, Duan L, et al. Diagnosis of liquid valve based on undecimated lifting scheme packet and singular value decomposition. Journal of Mechanical Engineering, 2011, 47(9): 72–77 (in Chinese)
7. Liu Y, Zhang J, Lin J, et al. Application of improved LMD, SVD technique and RVM to fault diagnosis of diesel valve trains. Transactions of Tianjin University, 2015, 21(4): 304–311
8. Yu Z, Sun Y, Jin W. A novel generalized demodulation approach for multi-component signals. Signal Processing, 2016, 118: 188–202
9. Zhao X, Ye B, Chen T. Difference spectrum theory of singular value and its application to the fault diagnosis of headstock of lathe. Journal of Mechanical Engineering, 2010, 46(1): 100–108 (in Chinese)
10. Zhong Z, Zhang B, Durrani T S, et al. Nonlinear signal processing for vocal folds damage detection based on heterogeneous sensor network. Signal Processing, 2016, 126(S1): 125–133
11. Zeng M, Yang Y, Zheng J, et al. μ-SVD based denoising method and its application to gear fault diagnosis. Journal of Mechanical Engineering, 2015, 51(3): 95–103 (in Chinese)
12. Zhu S, Qiao Z, Yang Z. An improved method for the extraction of weak signal based on SVD and EMD. Measurement & Control Technology, 2014, 33(1): 60–62
13. Jiang W, Zheng Z, Zhu Y, et al. Demodulation for hydraulic pump fault signals based on local mean decomposition and improved adaptive multiscale morphology analysis. Mechanical Systems and Signal Processing, 2015, 58–59: 179–205
14. Sun W, Xiong B, Huang J, et al. Fault diagnosis of a rolling bearing using wavelet packet de-noising and LMD. Journal of Vibration and Shock, 2012, 31(18): 153–156 (in Chinese)
15. Morzfeld M, Ajavakom N, Ma F. Diagonal dominance of damping and the decoupling approximation in linear vibratory systems. Journal of Sound and Vibration, 2009, 320(1–2): 406–420
16. Wu Z, Cheng J, Yu Y, et al. Adaptive characteristic-scale decomposition method and its application. China Mechanical Engineering, 2015, 42(23): 7–15 (in Chinese)
17. Wang B, Ren Z, Wen B. Fault diagnoses method of rotating machines based on nonlinear. Chinese Journal of Mechanical Engineering, 2012, 48(5): 63–69
18. Cao L. Practical method for determining the minimum embedding dimension of a scalar time series. Physica D: Nonlinear Phenomena, 1997, 110(1–2): 43–50
19. Miao L, Ren W, Hu Y, et al. Separating temperature effect from dynamic strain measurements of a bridge based on analytical mode decomposition method. China Mechanical Engineering, 2012, 31 (21): 6–10 (in Chinese)
20. Wang H, Li X, Wang G, et al. Research on failure of wind turbine gearbox and recent development of its design and manufacturing technologies. China Mechanical Engineering, 2013, 24(11): 1542–1549 (in Chinese)
21. Vanhollebeke F, Peeters P, Helsen J, et al. Large scale validation of a flexible multibody wind turbine gearbox model. Journal of Computational and Nonlinear Dynamics, 2015, 10(4): 041006